

# Assessment of cerebral microbleeds by susceptibility-weighted imaging in Alzheimer's disease patients: A neuroimaging biomarker of the disease

Gianvincenzo Sparacia<sup>1</sup>, Francesco Agnello<sup>1</sup>, Giuseppe La Tona<sup>1</sup>,  
Alberto Iaia<sup>2</sup>, Federico Midiri<sup>1</sup> and Benedetta Sparacia<sup>3</sup>

## Abstract

**Purpose:** The objective of this study was to correlate the presence and distribution of cerebral microbleeds in Alzheimer's disease patients with cerebrospinal fluid biomarkers (amyloid-beta and phosphorylated tau 181 protein levels) and cognitive decline by using susceptibility-weighted imaging magnetic resonance sequences at 1.5 T.

**Material and methods:** Fifty-four consecutive Alzheimer's disease patients underwent brain magnetic resonance imaging at 1.5 T to assess the presence and distribution of cerebral microbleeds on susceptibility-weighted imaging images. The images were analyzed in consensus by two neuroradiologists, each with at least 10 years' experience. Dementia severity was assessed with the Mini-Mental State Examination score.

A multiple regression analysis was performed to assess the associations between the number and location of cerebral microbleed lesions with the age, sex, duration of the disease, cerebrospinal fluid amyloid-beta and phosphorylated tau 181 protein levels, and cognitive functions.

**Results:** A total of 296 microbleeds were observed in 54 patients; 38 patients (70.4%) had lobar distribution, 13 patients (24.1%) had non-lobar distribution, and the remaining three patients (5.6%) had mixed distribution, demonstrating that Alzheimer's disease patients present mainly a lobar distribution of cerebral microbleeds.

The age and the duration of the disease were correlated with the number of lobar cerebral microbleeds ( $P < 0.001$ ).

Cerebrospinal fluid amyloid-beta, phosphorylated tau 181 protein levels, and cognitive decline were correlated with the number of lobar cerebral microbleeds in Alzheimer's disease patients ( $P < 0.001$ ).

**Conclusion:** Lobar distribution of cerebral microbleeds is associated with Alzheimer's disease and the number of lobar cerebral microbleeds directly correlates with cerebrospinal fluid amyloid-beta and phosphorylated tau 181 protein levels and with the cognitive decline of Alzheimer's disease patients.

## Keywords

Cerebral microbleeds, susceptibility-weighted imaging, Alzheimer's disease, magnetic resonance imaging

## Introduction

Alzheimer's disease (AD) is a progressive neurodegenerative disorder that affects the brain in adult patients who typically remain asymptomatic for a considerable duration of time before demonstrating clinical evidence of cognitive decline.<sup>1,2</sup>

Cerebral amyloid angiopathy (CAA) is commonly observed in pathology analysis of AD-affected brains and it is associated with lobar distribution of cerebral microbleeds (CMBs), which affect cognitive function.<sup>3–5</sup>

CMBs are presumed to reflect focal hemosiderin deposits in the brain that are caused by leakage of red blood cells from small blood vessels.<sup>6,7</sup>

CMBs can be visualized on T2\*-weighted gradient-recalled-echo (GRE) magnetic resonance (MR)

imaging sequences, as small foci of decreased signal intensity.<sup>3,8</sup>

In recent years, the introduction of susceptibility-weighted imaging (SWI) MR sequences has improved CMB detection in MR imaging.

<sup>1</sup>DIBIMED – Sezione di Scienze Radiologiche, Università degli Studi di Palermo, Italy

<sup>2</sup>Neuroradiology Section, Christiana Care Health System, USA

<sup>3</sup>PROSAMI, Università degli Studi di Palermo, Italy

## Corresponding author:

Gianvincenzo Sparacia, DIBIMED – Sezione di Scienze Radiologiche  
Università degli Studi di Palermo Via Del Vespro 127, 90127 Palermo, Italy.  
Email: gianvincenzo.sparacia@unipa.it

The SWI sequence is a velocity compensated high-resolution 3D gradient-echo sequence that uses magnitude and filtered-phase information to create a new contrast.<sup>9–11</sup> As a result, CMBs are more sensitively detected by SWI compared with T2\*-weighted GRE.<sup>3,12–14</sup>

A previous study<sup>4</sup> based on 3 T MR imaging and T2\* GRE sequence demonstrated an association between lobar distributed CMBs and cerebrospinal fluid (CSF) amyloid-beta ( $A\beta$ ) levels as well as with CSF phosphorylated tau 181 protein (p-tau) levels and the presence of cognitive decline in AD patients.

The aim of this study was to assess the presence and distribution of CMBs with SWI MR sequences implemented in a more widely available 1.5 T MR unit and to correlate the presence and distribution of CMBs with CSF biomarkers of AD and with cognitive decline in AD patients.

## Material and methods

### Patient population

We included 54 consecutive patients (20 men, 34 women; mean age:  $76.8 \pm 5.2$  years) diagnosed as having AD (mean duration of the disease:  $7.2 \pm 3.7$  years).

The diagnosis was established according to the criteria for probable AD as proposed by the National Institute of Neurological and Communicative Disorders and Stroke and the Alzheimer's Disease and Related Disorders Association.<sup>15</sup>

Exclusion criteria were: previous stroke or head trauma; cancer history; severe cardiac, renal, or hepatic disease; recent history of infection or inflammatory disease. Dementia severity was assessed with the Mini-Mental State Examination.<sup>16</sup> Demographic data are presented in Table 1.

Patients underwent lumbar puncture to obtain CSF samples for quantifying levels of CSF  $A\beta$  and p-tau.

The institutional review board of our institution approved this retrospective study and written informed consent was obtained from all patients.

### MR imaging

All patients underwent MR examination between January 2015 and May 2016. All MR examinations

were performed on a 1.5 T MR scanner (Achieva, Philips Medical Systems, Best, The Netherlands).

MR imaging protocol included axial and sagittal fast-spin echo (FSE) T2W (5100/110 [TR/TE]) images, axial fluid-attenuated inversion-recovery (FLAIR) (8000/140/2400 [TR/TE/TI]) images, along with axial, sagittal, and coronal non-enhanced and contrast-enhanced (0.1 mmol/Kg gadobutrol - Gadovist, Bayer, Germany) FSE T1W (650/15 [TR/TE]) images with a field of view (FOV) of 22 cm, matrix  $512 \times 512$ , slice thickness 5 mm, intersection gap 1 mm, number of excitations 2.

Susceptibility weighted imaging (SWI) sequences were obtained using a technique that combines a long-TE high-resolution fully flow-compensated 3D GRE sequence with filtered phase information in each voxel, as previously described.<sup>9–11</sup>

The SWI images (3D GRE 24/34 [TR/TE], flip angle  $10^\circ$ ) were obtained with a FOV of 22 cm, matrix  $256 \times 512$ , slice thickness 1.2 mm, gap 0 mm, number of excitations 1 and acquisition time 5.15 min. Subsequently, the SWI sequences were reconstructed to obtain images of 5 mm thickness, 1 mm intersection gap, oriented in the axial plane similar to that of FSE images.

Calcifications of the basal ganglia and deep cerebellar nuclei were considered as normal findings if present and not taken into account during the review of the images. None of the patients had disorders of calcium/phosphate metabolism.

### Image analysis

The images were analyzed in consensus by two neuroradiologists, each with at least 10 years experience.

Images, presented in random order, were analyzed for the presence and location of the CMB lesions.

CMBs were defined as small hypointense lesions within the brain parenchyma that measured less than 10 mm on the SWI images.

The locations of the microbleeds were subdivided into: non-lobar, if located in the basal ganglia, thalami, brain stem, or cerebellum; lobar, if located in one of the four cerebral lobes: frontal, parietal, occipital, and temporal; mixed, in the case of CMBs distributed in both lobar and non-lobar locations.

The two neuroradiologists recorded the location and number of lesions seen on SWI images on a PACS system (Agfa HealthCare GmbH - Bonn).

### Statistical analysis

The ordinary least-squares multiple regression analysis was performed to assess the associations between the number and location of CMB lesions (dependent variable) with the patient's age and sex, duration of the disease, CSF  $A\beta$ , p-tau levels, and cognitive functions (independent variables). Differences for a  $P$  value of  $< .05$  were considered statistically significant. Statistical analysis was performed using the statistical software package SPSS (SPSS, Chicago, IL).

**Table 1.** Characteristics of AD patients.

Variables	Number
Number of patients	54
Mean age ( $\pm$ SD), years	$76.8 (\pm 5.2)$
Sex, male/female	20/34
Mean duration of AD ( $\pm$ SD), years	$7.2 (\pm 3.7)$
MMSE score ( $\pm$ SD)	$18.3 (\pm 8.5)$

AD: Alzheimer's disease; MMSE: Mini-Mental State Examination.

## Results

CMBs were demonstrated as small, rounded, hypointense lesions within the brain parenchyma that measured less than 10 mm on the SWI images.

A total of 296 microbleeds were observed in 54 patients; 38 patients (70.4%) had lobar distribution, 13 patients (24.1%) had non-lobar distribution and the remaining three patients (5.6%) had mixed distribution (see Table 2 and Figures 1–3).

The mean count of microbleeds was 5.4 per patient and the median was four CMBs per patient. The frequency of the number of CMBs was as follow: seven patients (13%) had one microbleed, 11 patients (20.4%) had two microbleeds, eight patients (14.8%) had three microbleeds, eight patients (14.8%) had four microbleeds, four patients (7.4%) had five microbleeds and the remaining 16 patients (29.6%) had more than five microbleeds (Table 3).

The correlation analysis showed that the age of the patients and the duration of the disease were

significantly correlated with the number of lobar CMBs ( $P < 0.001$ , age coefficient .46, duration of the disease coefficient .58).

A significant correlation was found between the CSF  $A\beta$  levels and the number of lobar CMBs ( $P < 0.001$ , coefficient  $-.32$ ).

Non-lobar microbleeds were not associated with CSF  $A\beta$  levels.

A direct correlation was found between the number of lobar CMBs and CSF p-tau levels ( $P < 0.001$ , coefficient .35).

Non-lobar microbleeds were not correlated with CSF p-tau levels.

Using a generalized linear mixed-effects model adjusted for covariates, including CSF  $A\beta$  levels, age, sex, and disease duration, the number of lobar microbleeds was significantly associated with the MMSE score ( $P < 0.001$ , coefficient  $-.37$ ).

Non-lobar microbleeds were not associated with change in MMSE score ( $P < 0.001$ ). Results are summarized in Table 4.

**Table 2.** Number of CMBs subdivided by location.

Location	Number of patients	Number of CMBs	%
Lobar	38	238	70.4
Non-lobar	13	46	24
Mixed	3	12	5.6
Total	54	296	100

Location: Lobar – CMBs located in one of the four cerebral lobes: frontal, parietal, occipital, and temporal; Non-lobar – CMBs located in the basal ganglia, thalami, brain stem, or cerebellum; Mixed – mixed distribution of the CMBs in both lobar and non-lobar locations.

CMBs: cerebral microbleeds.

## Discussion

The results of our study confirm that lobar distribution of microbleeds is associated with AD as reported in previous publications.<sup>17,18</sup> In particular, of the 54 AD patients reviewed, 38 (70.4%) had a lobar distribution of the microbleeds, 13 (24.1%) had a non-lobar distribution and the remaining three (5.6%) had a mixed distribution (Table 2).

In accordance with results of previous publications, which showed lower CSF  $A\beta$  levels in AD patients with lobar microbleeds,<sup>4,19,20</sup> we likewise found a significant correlation between CSF  $A\beta$  levels and the number of lobar CMBs ( $P < 0.001$ , coefficient  $-.32$ ), which means

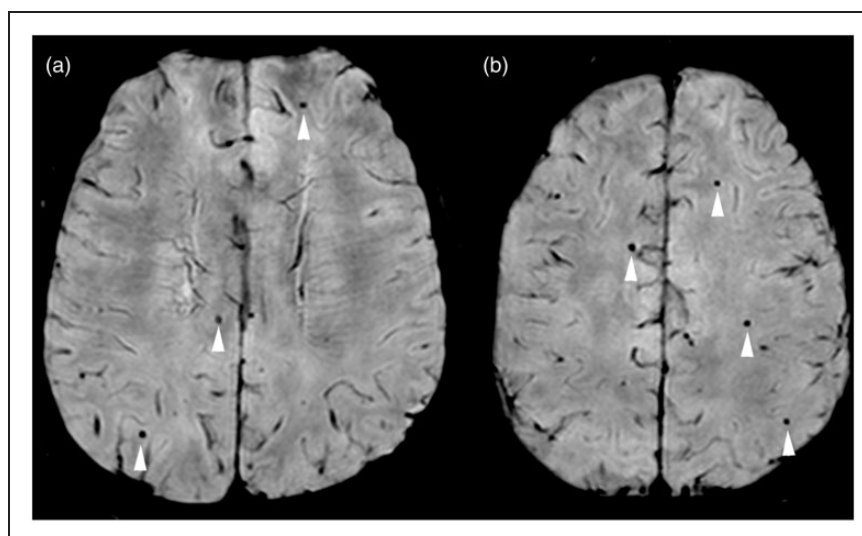


**Figure 1.** Lobar distributed cerebral microbleeds in Alzheimer's disease patient. (ab) Axial SWI MR images show multiple small, rounded, hypointense cerebral microbleeds bilaterally in the parietal and frontal lobes (arrowhead). SWI: susceptibility-weighted imaging; MR: magnetic resonance.

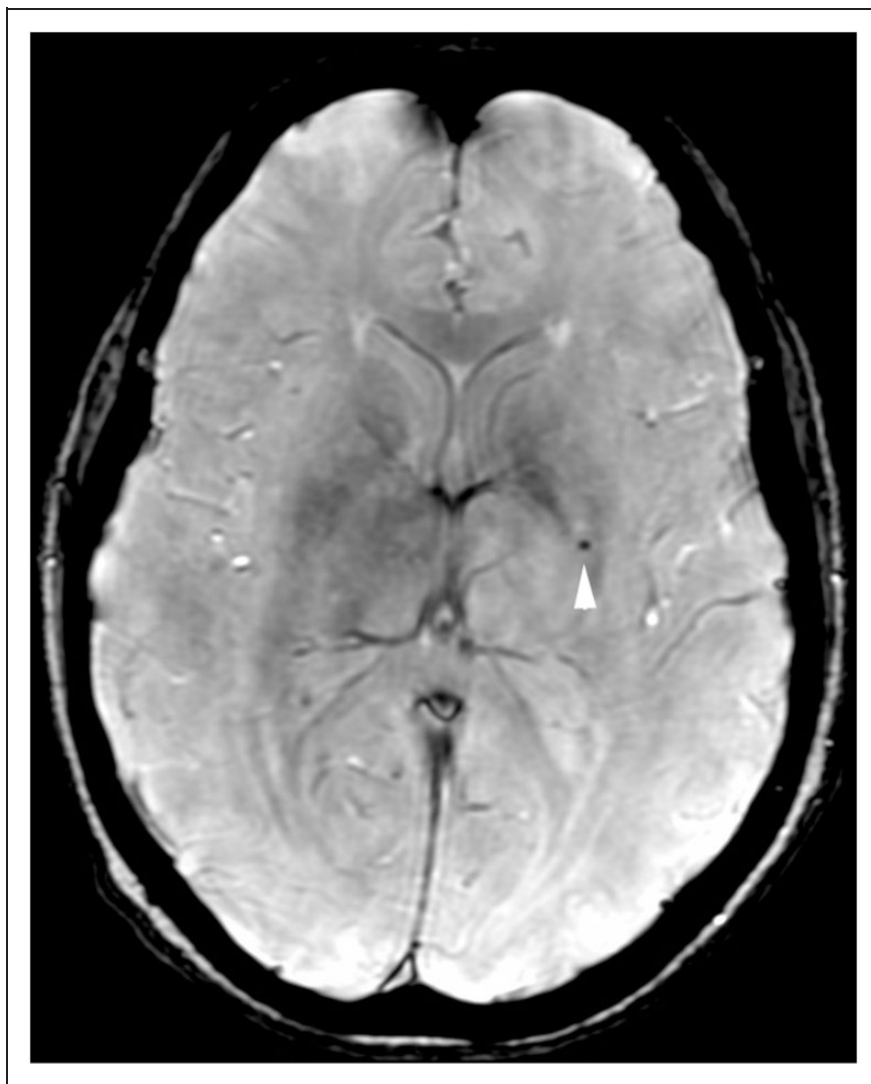


**Figure 2.** Non-lobar distributed cerebral microbleed in Alzheimer's disease patient. Axial SWI MR image shows a small, rounded, hypointense cerebral microbleed in the left basal ganglia (arrowhead). SWI: susceptibility-weighted imaging; MR: magnetic resonance.

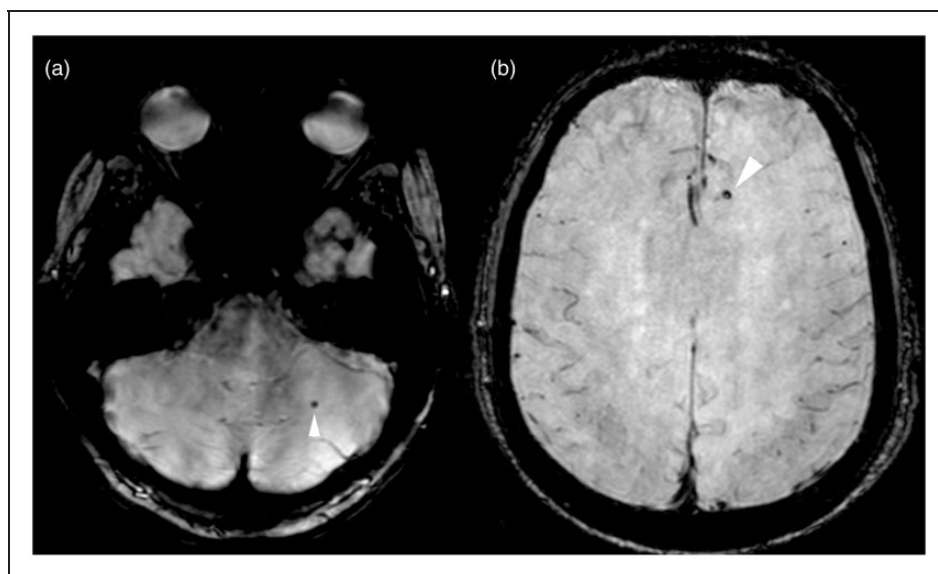


**Figure 3.** Mixed distribution of cerebral microbleeds in Alzheimer's disease patient. (ab) Axial SWI MR images show small, rounded, hypointense cerebral microbleeds in the (a) left cerebellar hemisphere and in the (b) left frontal lobe (arrowhead). SWI: susceptibility-weighted imaging; MR: magnetic resonance.



**Table 3.** Frequency of the number of CMBs seen on SWI sequence in AD patients.

Number of CMBs	Number of patients	Total number of CMBs	%
1	7	7	13.0
2	11	22	20
3	8	24	14.8
4	8	32	14.8
5	4	20	7.4
6	3	18	5.6
7	1	7	1.9
8	2	16	3.7
9	1	9	1.9
11	1	11	1.9
12	1	12	1.9
13	1	13	1.9
14	2	28	3.7
17	1	17	1.9
18	1	18	1.9
21	2	42	3.7
Total	54	296	100.0

SWI: susceptibility-weighted imaging; AD: Alzheimer's disease; CMBs: cerebral microbleeds.

**Table 4.** Association of number of CMBs with age, duration of AD, CSF biomarkers, and cognitive function measured with MMSE score.

Variables	Coefficient	P value
Age	.46	$P < 0.001$
Duration of AD	.58	$P < 0.001$
CSF A $\beta$ level	-.32	$P < 0.001$
CSF p-tau level	.35	$P < 0.001$
MMSE score	-.37	$P < 0.001$

CMBs: cerebral microbleeds; AD: Alzheimer's disease; CSF: cerebrospinal fluid; A $\beta$ : amyloid-beta; p-tau: phosphorylated tau 181 protein; MMSE: Mini-Mental State Examination.

that greater brain amyloidosis is associated with increasing numbers of lobar CMBs.

It should be noted that previous investigators<sup>4</sup> were unable to establish statistical significance for this correlation. A possible explanation for the significant correlation found in our study may relate to a substantial technical difference between the studies, as we used SWI sequences as opposed to the T2\* GRE sequences used by others. SWI sequences have been demonstrated to be superior to T2\* GRE sequences, the former having higher sensitivity in demonstrating CMBs.<sup>21,22</sup> Such increased sensitivity of SWI for visualization of CMBs probably leads to detection of a greater number of microbleeds in our study and thus accounts for the statistically significant correlation with the lower CSF A $\beta$  levels observed in our AD patients.

An association between lobar microbleeds and elevated CSF p-tau level was also demonstrated ( $P < 0.001$ , coefficient .35), implying that a larger number of lobar CMBs are observed in patients with higher CSF p-tau levels. This correlation may reflect the notion that microbleeds are the imaging expression of damaged microvasculature, or that CMBs may lead to cerebral inflammation, which results in increased tau pathology.<sup>4,23</sup>

Non-lobar microbleeds were not associated with CSF A $\beta$  and p-tau levels.

The patient's age and the duration of the disease were correlated with the number of lobar CMBs ( $P < 0.001$ , age coefficient .46, duration of the disease coefficient .58), and a correlation analysis adjusted for CSF A $\beta$  levels, age, sex, and duration of the disease showed that the number of lobar microbleeds was significantly associated with the MMSE score, implying that worsening cognitive function is associated with the presence and number of lobar CMBs ( $P < 0.001$ , coefficient -.37).

This result confirms conclusions reached by previous publications which have shown a direct correlation between the extent of amyloid angiopathy and the degree of memory and cognitive decline in AD patients with lobar microbleeds.<sup>4,18,24,25</sup>

Non-lobar microbleeds were not associated with change in MMSE score ( $P < 0.001$ ), as demonstrated in previous studies.<sup>4,26</sup>

One of the limitations of our study is that it lacked a comparison between T2\* GRE sequences and SWI sequences in the detection of CMBs. However, this aspect was beyond the purpose of our study, as the higher sensitivity of SWI sequences for detection of CMBs had already been demonstrated by several previous publications.<sup>21,22</sup>

## Conclusion

Improved detection of CMBs with SWI sequences may contribute to more accurate identification of AD patients, who typically present a lobar distribution of CMBs.

The number of lobar CMBs is correlated to CSF A $\beta$  and p-tau levels and with the degree of cognitive decline of AD patients.

Our results should be carefully evaluated as our sample population was relatively homogeneous, resulting in limited generalizability, and further validation in a larger prospective population is required.

## Funding

This research received no specific grant from any funding agency in the public, commercial, or not-for-profit sectors.

## Conflict of interest

The authors declared no potential conflicts of interest with respect to the research, authorship, and/or publication of this article.

## References

1. Hebert LE, Scherr PA, Bienias JL, et al. Alzheimer disease in the US population: prevalence estimates using the 2000 census. *Arch Neurol* 2003; 60: 1119–1122.
2. Blennow K, de Leon MJ and Zetterberg H. Alzheimer's disease. *Lancet* 2006; 368: 387–403.
3. Nandigam RN, Viswanathan A, Delgado P, et al. MR imaging detection of cerebral microbleeds: effect of susceptibility-weighted imaging, section thickness, and field strength. *AJNR Am J Neuroradiol* 2009; 30: 338–343.
4. Chiang GC, Cruz Hernandez JC, Kantarci K, et al. Cerebral Microbleeds, CSF p-Tau, and Cognitive Decline: Significance of Anatomic Distribution. *AJNR Am J Neuroradiol* 2015; 36: 1635–1641.
5. Yates PA, Sirisriro R, Villemagne VL, Farquharson S, Masters CL and Rowe CC. Cerebral microhemorrhage and brain beta-amyloid in aging and Alzheimer disease. *Neurology* 2011; 77: 48–54.
6. Zhang JB, Li MF, Zhang HX, et al. Association of serum vascular endothelial growth factor levels and cerebral microbleeds in patients with Alzheimer's disease. *Eur J Neurol* 2016; 23: 1337–1342.
7. Vernooij MW, Ikram MA, Wielopolski PA, et al. Cerebral Microbleeds: Accelerated 3D T2\*-weighted GRE MR Imaging versus Conventional 2D T2\*-weighted GRE MR Imaging for Detection. *Radiology* 2008; 248: 272–277.
8. Fazekas F, Kleinert R, Roob G, et al. Histopathologic analysis of foci of signal loss on gradient-echo T2\*-weighted MR images in patients with spontaneous intracerebral hemorrhage: evidence of microangiopathy-related microbleeds. *AJNR Am J Neuroradiol* 1999; 20: 637–642.
9. Haacke EM, Mittal S, Wu Z, et al. Susceptibility-weighted imaging: technical aspects and clinical applications, part 1. *AJNR Am J Neuroradiol* 2009; 30: 19–30.
10. Mittal S, Wu Z, Neelavalli J, et al. Susceptibility-weighted imaging: technical aspects and clinical applications, part 2. *AJNR Am J Neuroradiol* 2009; 30: 232–252.
11. Sparacia G, Speciale C, Banco A, et al. Accuracy of SWI sequences compared to T2\*-weighted gradient echo sequences in the detection of cerebral cavernous malformations in the familial form. *Neuroradiol J* 2016; 29: 326–335.
12. Goos JD, van der Flier WM, Knol DL, et al. Clinical relevance of improved microbleed detection by susceptibility-weighted magnetic resonance imaging. *Stroke* 2011; 42: 1894–1900.
13. Mori N, Miki Y, Kikuta K, et al. Microbleeds in moyamoya disease: susceptibility-weighted imaging versus T2\*-weighted imaging at 3 Tesla. *Invest Radiol* 2008; 43: 574–579.
14. Guo LF, Wang G, Zhu XY, et al. Comparison of ESWAN, SWI-SPGR, and 2D T2\*-weighted GRE sequence for depicting cerebral microbleeds. *Clin Neuroradiol* 2013; 23: 121–127.
15. McKhann G, Drachman D, Folstein M, et al. Clinical diagnosis of Alzheimer's disease: report of the NINCDS-ADRDA Work Group under the auspices of Department of Health and Human Services Task Force on Alzheimer's Disease. *Neurology* 1984; 34: 939–944.
16. Folstein MF, Folstein SE and McHugh PR. 'Mini-mental state': a practical method for grading the cognitive state of patients for the clinician. *J Psychiatr Res* 1975; 12: 189–198.
17. Chung CP, Chou KH, Chen WT, et al. Strictly Lobar Cerebral Microbleeds Are Associated With Cognitive Impairment. *Stroke* 2016; 47: 2497–2502.
18. Shams S, Granberg T, Martola J, et al. Cerebral microbleeds topography and cerebrospinal fluid biomarkers in cognitive impairment. *J Cereb Blood Flow Metab* 2016; May 13; pii: 0271678X16649401.
19. Park JH, Seo SW, Kim C, et al. Pathogenesis of cerebral microbleeds: in vivo imaging of amyloid and subcortical ischemic small vessel disease in 226 individuals with cognitive impairment. *Ann Neurol* 2013; 73: 584–593.
20. Schrag M, McAuley G, Pomakian J, et al. Correlation of hypointensities in susceptibility-weighted images to tissue histology in dementia patients with cerebral amyloid angiopathy: a postmortem MRI study. *Acta Neuropathol* 2010; 119: 291–302.
21. Shams S, Martola J, Cavallin L, et al. SWI or T2\*: Which MRI Sequence to Use in the Detection of Cerebral Microbleeds? The Karolinska Imaging Dementia Study. *AJNR Am J Neuroradiol* 2015; 36: 1089–1095.
22. Ayaz M, Boikov AS, Haacke EM, et al. Imaging cerebral microbleeds using susceptibility weighted imaging: one step toward detecting vascular dementia. *J Magn Reson Imaging* 2010; 31: 142–148.
23. Williams S, Chalmers K, Wilcock GK, et al. Relationship of neurofibrillary pathology to cerebral amyloid angiopathy in Alzheimer's disease. *Neuropathol Appl Neurobiol* 2005; 31: 414–421.
24. Miwa K, Tanaka M, Okazaki S, et al. Multiple or mixed cerebral microbleeds and dementia in patients with vascular risk factors. *Neurology* 2014; 83: 646–653.
25. Arvanitakis Z, Leurgans SE, Wang Z, et al. Cerebral amyloid angiopathy pathology and cognitive domains in older persons. *Ann Neurol* 2011; 69: 320–327.
26. Gregoire SM, Scheffler G, Jäger HR, et al. Strictly lobar microbleeds are associated with executive impairment in patients with ischemic stroke or transient ischemic attack. *Stroke* 2013; 44: 1267–1272.